Available online at www.sciencedirect.com

ScienceDirect

Physics Procedia 69 (2015) 503 – 508

Physics Procedia

10th World Conference on Neutron Radiography 5-10 October 2014

Visualization and Measurement of Adsorption/Desorption Process of Ethanol in Activated Carbon Adsorber

Hitoshi Asano[a,] *, Kenta Murata[a], Nobuyuki Takenaka[a], Yasushi Saito[b]

[a] *Department of Mechanical Engineering, Kobe University, 1-1, Rokkodai, Nada, Kobe 657-8501, Japan,*
[b] *Kyoto University Research Reactor Institute, 2 Asashiro-Nishi, Kumatori, Osaka 590-0494, Japan*

Abstract

Adsorption refrigerator is one of the efficient tools for waste heat recovery, because the system is driven by heat at relative low temperature. However, the coefficient of performance is low due to its batch operation and the heat capacity of the adsorber. In order to improve the performance, it is important to optimize the configuration to minimize the amount of driving heat, and to clarify adsorption/desorption phenomena in transient conditions. Neutron radiography was applied to visualize and measure the adsorption amount distribution in an adsorber. The visualization experiments had been performed at the neutron radiography facility of E-2 port of Kyoto University Research Reactor. Activated carbon and ethanol were used as the adsorbent and refrigerant. From the acquired radiographs, adsorption amount was quantitatively measured by applying the umbra method using a checkered neutron absorber with boron powder. Then, transient adsorption and desorption processes of a rectangular adsorber with 84 mm in width, 50 mm in height and 20 mm in depth were visualized. As the result, the effect of fins in the adsorbent layer on the adsorption amount distribution was clearly visualized.

Selection and peer-review under responsibility of Paul Scherrer Institut

Keywords: Adsorption, Nondistructive measurement, Activated carbon, Ethanol, Neutron radiography

1. Introduction

An adsorption refrigerating system is expected to be one of the efficient tools for waste heat recovery, because the system can be driven by heat at relative low temperature. The operation of an adsorption refrigerator is

* Corresponding author. Tel.: +81-78-803-6122; fax: +81-78-803-6122.
E-mail address: asano@mech.kobe-u.ac.jp

Selection and peer-review under responsibility of Paul Scherrer Institut
doi:10.1016/j.phpro.2015.07.071

explained with Fig. 1. The evaporative pressure is kept low by adsorbing vapor into the adsorber. Since adsorbed amount in equilibrium increase with decreasing the temperature, and condensation heat is released in adsorption process, the adsorbent should be cooled to keep the adsorption performance. After the adsorption process, the adsorber is connected to a condenser by a valve switching. Then, the vapor is regenerated by heating of the adsorbent. The input heat is used for temperature rise of the adsorbent and the container, and is also used for the vaporization heat of refrigerant.

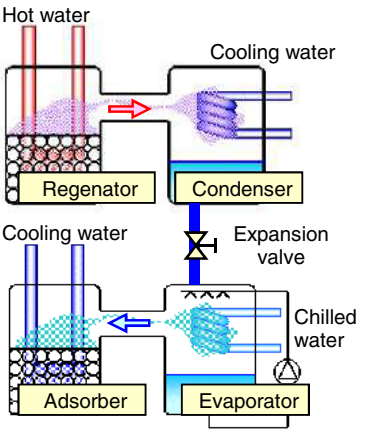

Fig.1 Schematic diagram of adsorption refrigerator.

The important point to improve the coefficient of performance is to enhance heat diffusion in the adsorption bed. Metallic fins or high thermal conductive fivers are often installed in adsorbent bed to enhance the heat diffusion. However, since an increase in heat capacity of the adsorber leads to a lowering of the coefficient of performance due to its batch operation, the configuration of adsorber must be optimized to minimize the amount of driving heat. On the other hand, higher bulk density of adsorbent will lead to higher heat diffusion. However, higher bulk density means smaller porosity and causes larger flow resistance of vapor. The fact will lead to a decrease in adsorption rate. Therefore, it is required for the optimization of the structure of adsorber to know the distribution of adsorbed refrigerant inside the adsorbent bed during adsorption or desorption. Numerical simulation models had been constructed by Kariya, et al. (2007), Zhao, et al. (2012), and Yang (2009). These models are based on some assumptions, for example, a homogenous distribution of adsorbent particles and a constant heat resistance between metallic wall and adsorbent particles. Measurement of adsorbed refrigerant distribution inside an adsorbent bed during transient process is required not only for the understanding of the phenomena but also for the benchmark data for such numerical simulation model. Neutron radiography is very effective to visualize fluid with hydrogen in a solid material, since the attenuation coefficient of neutron beam for hydrogen is higher than that for many other materials. For example, the attenuation coefficient for water and ethanol is quite higher than aluminum, copper, and iron. Asano, et al. (2005, 2007) had carried out visualization experiments for hygroscopic water distribution in silica gel particle bed. Wet particles were packed in an aluminum cylinder, then transient water distributions in desorption process with heating was successfully visualized. A cylindrical adsorption unit cell using silica gel particles could be successfully visualized by neutron radiography. Cross-sectional distributions could be measured from multidirectional projection image by a CT method.

In this study, adsorbed refrigerant distributions in an adsorbent bed were visualized by Neutron radiography for activated carbon powder and ethanol pair adsorber. Amount of adsorbed ethanol inside adsorbent in a rectangular container with aluminum fins was quantitatively measured by applying the umbra method using a checked neutron adsorber during transient adsorption or desorption process.

2. Quantitative measurement by the umbra method

The experiments were performed in the neutron radiography facility at the E2 port of Kyoto University Research Reactor. Attenuated neutron beam was converted to optical image on the scintillation convertor, and the image was taken by a cooled CCD camera with 4008×2672 image elements and 16 bit intensity level. The pixel size was 42 μm in this experiment. Assuming that the brightness of a visualized image is proportional to the beam intensity on a scintillation converter and neglecting the attenuation in the vapor refrigerant in the adsorption bed, the brightness of the adsorbent bed in a metallic container $S(x, y, t)$ is expressed as

$$S(x,y,t)=G(x,y)I_0(x,y)\exp\left(-\rho_w\mu_{m,w}t_w(x,y)-\rho_{Ad}\mu_{m,Ad}t_{Ad}(x,y)-\rho_r\mu_{m,r}t_r(x,y,t)\right)+O(x,y,t)$$

where G and O is the gain and offset of the imaging system, I_0 is the irradiated beam intensity, ρ, μ_m, and t are density, mass attenuation coefficient, and thickness along the neutron beam, respectively. The subscripts of w, Ad,

and r mean the wall, adsorbent, and refrigerant, respectively. The offset is caused by neutron scattering, stray light in the camera system, and dark current of the camera. Therefore, the value must be affected by the condition of the object.

In this study, the offset was measured by the umbra method proposed by Takenaka, et al. (2001). The validity of the method was confirmed from the measurements of liquid refrigerant and adsorbent steps with several thickness. The steps were made in aluminum container as shown in Fig. 2. In the measurement of adsorbent bed, the neutron radiographs were taken for the dry and equilibrium adsorption condition, and then adsorbed refrigerant thickness was calculated from the comparison between two radiographs. A checked B_4C grid with 3 mm in the pitch was placed at the front of the object to obtain umbra of neutron beam. An example original radiograph of the step of adsorbent layer in the equilibrium adsorption condition with the checked grid is shown in Fig. 2. The offset at a visualized area was obtained by interpolation of the brightness at adjacent parts of umbra. Activated carbon powder and ethanol was used as the adsorbent and refrigerant, respectively. The measured values of $\rho\mu_m t$ are plotted against the thickness of liquid ethanol as shown in Fig. 3. Bold symbols show the compensated results by the umbra method. Since the density and mass attenuation coefficient is constant, the relation must be linear. It was confirmed that the mass attenuation coefficient of liquid ethanol could be measured by the umbra method, and the value was 3.86 cm^2/g. For the adsorbent bed, it could be seen that the compensation was required for the quantitative measurement. Using the measured attenuation coefficient the amount of adsorbed refrigerant in equilibrium condition was calculated and compare with the experimentally measured values by El-Sharkawy, et al. (2009) as shown in Fig. 4. The measured values by neutron radiography were agreed well with the previous results.

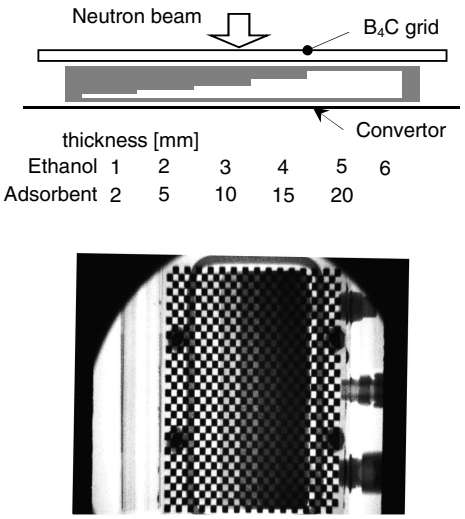

Fig. 2 Neutron radiograph of adsorbent step with checked B_4C grid, and the configuration.

3. Measurements of adsorption/desorption process

Transient changes in distribution of adsorbed ethanol were visualized during the adsorption or desorption process. Schematic diagram of the experimental setup and the configuration of the adsorbent container are shown in Fig. 5 and Fig. 6, respectively. The container was connected to a liquid ethanol reservoir immersed in a temperature controlled water. The vapor pressure was maintained

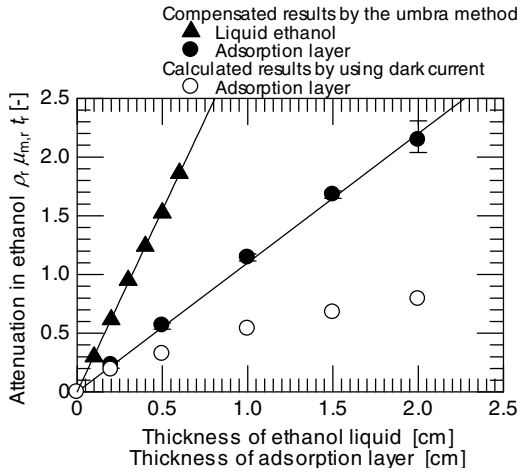

Fig. 3 Attenuation characteristic of liquid ethanol and adsorbent bed.

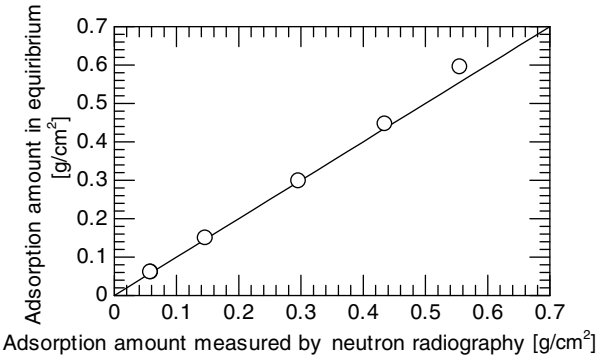

Fig. 4 Comparison in adsorption amount of liquid ethanol in activated carbon particle bed.

by the water temperature. The container was made from aluminum. The inside depth was 20 mm. A water channel was drilled in the bottom wall. The adsorbent bed could be heated or cooled from the bottom wall. On the inner surface of the bottom wall, two aluminum fins with 1 mm in thickness were installed to enhance the heat diffusion in the adsorbent bed. The front and back walls were thin SUS plate with 0.5 mm in thickness to avoid heat diffusion through the walls. Temperatures were measured by the inserted thermocouples at four points shown in Fig. 6.

Examples of visualized results are shown in Figs 7. Exposure time and pixel size was 30 seconds and 42 μm, respectively. The reservoir temperature and the cooling water temperature were set to 10 and 30 ºC for the adsorption process, respectively. For the desorption process, those were 20 and 80 ºC. In the visualized images, the darker part means higher adsorbed amount. The inside wall and fin surface are traced by thin solid lines. For the dry condition in Fig. 6 (a), the adsorbent could be clearly visualized. Figure 6 (b) was taken in an adsorption process after 8 minutes from the start. Adsorption amount was larger in the surface layer and around the fins and sidewalls (area A) due to the effective cooling, and was also larger in the area C around the thermocouples. Flow resistance of vapor might be lower along the insert thermocouples due to the larger porosity. On the other hand, adsorption amount in the bottom area of the bed (area B) was smaller. The reason might be the existence of inert gas. In the desorption process, voids were observed on the bottom surface just after the start (area D in Fig. 7 (c), (i)). The voids might be caused by a strong vapor generation by heating. Then, the desorption progressed at a faster rate near the heat transfer surface (area E in Fig. 7 (c), (i)).

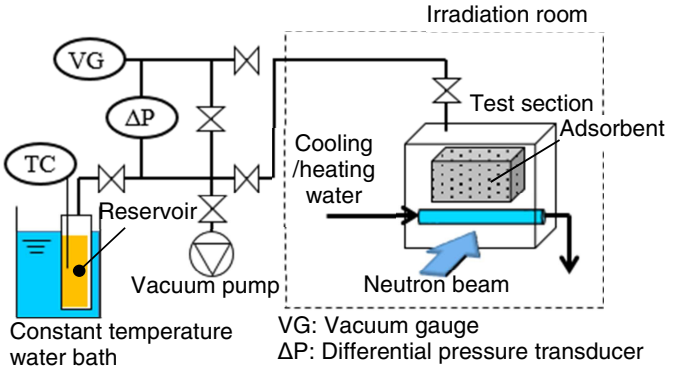

Fig. 5 Schematic diagram of experimental setup

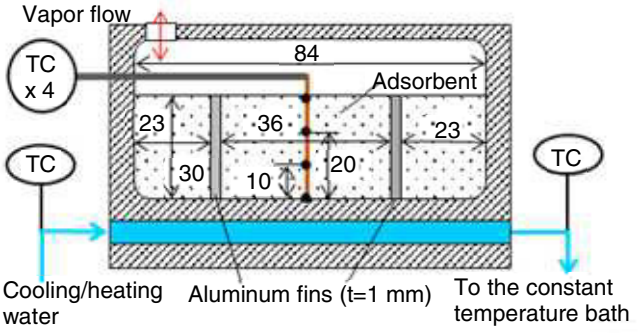

Fig. 6 Configuration of the test section

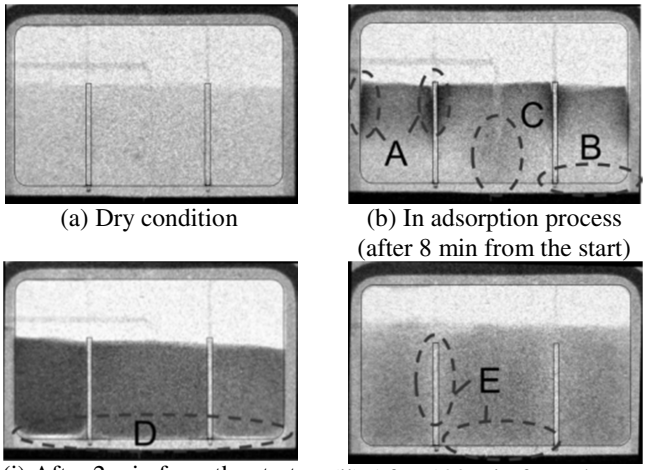

(a) Dry condition

(b) In adsorption process (after 8 min from the start)

(i) After 2 min from the start

(ii) After 120 min from the start

(c) Desorption process from the adsorption equilibrium.

Fig. 7 Visualized images by neutron radiography.

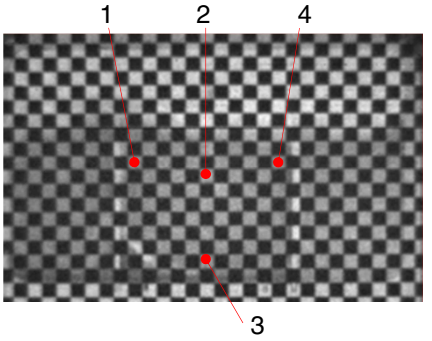

Fig. 8 Visualized image with checked B_4C grid.

Figure 8 shows a visualized image with the checked B_4C neutron adsorber. The adsorber was placed at the front of the test section. Adsorption amount at the visualized section indicated as 1 to 4 were measured during an adsorption process. At the initial condition, the activated carbon was perfectly dry. Time variations of temperatures and adsorption amount are plotted in Fig. 9 (a) and (b), respectively. The adsorbent bed temperature immediately increased after the start, and reached 70 ºC due to the strong adsorption. Then, the adsorption temperature gradually decreased, and the adsorption amount gradually increased with decreasing the temperature. It could be seen that the adsorption process was dominated by heat diffusion in the adsorbent bed. Adsorption amount was larger at the part of 1, 3, and 4 near the heat transfer surface including the aluminum fin.

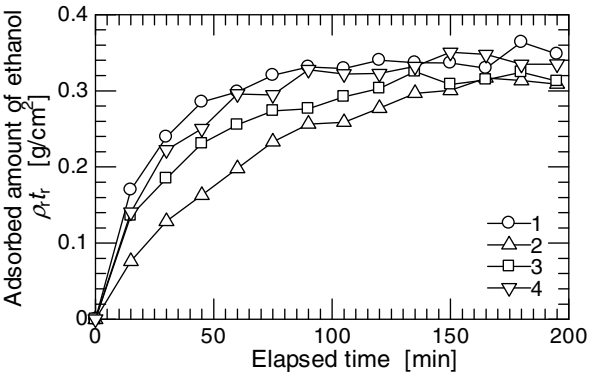

(a) Adsorption amount

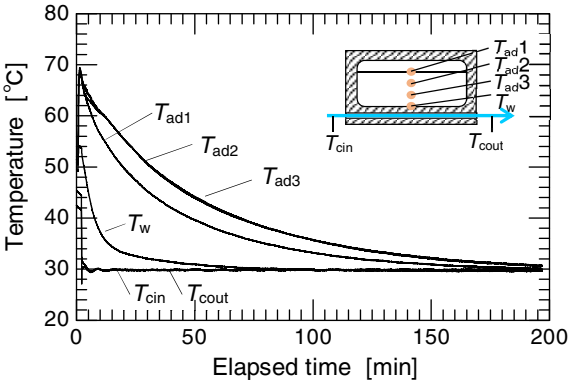

(b) Temperature

Fig. 9 Transient change in adsorption amount and temperature during adsorption process.

4. Conclusions

The adsorbed ethanol distribution in the activated carbon particle bed during adsorption and desorption process could be successfully visualized by neutron radiography. It was confirmed that the adsorbed amount could be quantitatively measured from radiographs by applying the umbra method to correct neutron scattering effect.

Acknowledgements

We would like to acknowledge Kyoto University Research Reactor Institute for supporting this study.

References

Asano, H., Nakajima, T., Takenaka, N., Fujii, T., 2005, Visualization of the Hygroscopic Water Distribution in an Adsorbent Bed by Neutron Radiography, Nuclear Instruments and Methods in Physics Research Section A, 542(1–3), 241–247.

Asano, H., Nakajima, T., Takenaka, N., 2007, Visualization and Measurement of Hygroscopic Water Distribution in a Unit Cell of Silica-Gel Adsorber by Neutron Radiography, Journal of Chemical Engineering Japan, 40(13), 1292–1297.

El-Sharkawy, I.I., Hassan, M., Saha, B.B., Koyama, S., Nasr, M.M., 2009, Study on Adsorption of Methanol onto Carbon Based Adsorbents, International Journal of Refrigeration, 32, 1579–1586

Kariya, K, Kuwahara, K., Koyama, S., 2007, Numerical Analysis for Optimal Design of Fin and Tube Type Adsorber - Case of activated carbon fiber/ethanol pair -, Transaction of the JSRAE, 24(4), 485–494. (in Japanese)

Takenaka, N., Asano, H., Fujii, T., Matsubayashi, M., 2001, A Method for Quantitative Measurement by Thermal Neutron Radiography, Nondestructive Testing and Evaluation, 16, 345–354.

Yang, P.Z., 2009, Heat and Mass Transfer in Adsorbent Bed with Consideration of Non-Equilibrium Adsorption, Applied Thermal Engineering, 29, 3198–3203.

Zhao, Y, Hu, E, Blazewicz, A., 2012, Dynamic Modelling of an Activated Carbon–Methanol Adsorption Refrigeration Tube with Considerations of Interfacial Convection and Transient Pressure Process, Applied Energy, 95, 276–284.